Solvation for Ions and Counterions: Complementary Relation between Ion−Counterion and Ion−Solvent Interaction

Shunsuke Mochizuki[†] **and Akihiro Wakisaka***

National Institute of Advanced Industrial Science and Technology (AIST), Onogawa 16-1,
Tsukuba, Ibaraki 305-8569, Japan

Received: December 18, 2001; In Final Form: March 5, 2002

The microscopic environments around a cation and its counterion were experimentally studied for methanol solutions of CsCl, LiCl, LiI, and $LiClO_4$ through mass spectrometric analysis of clusters generated from solutions. The change of the microscopic environments around cations and counteranions induced by the addition of 18-crown-6 were directly observed, which confirmed complementary relation between the ion−counterion and the ion−solvent interaction, as a representative solution property. For CsCl and LiCl solutions, by the addition of 18-crown-6, the solvated cation clusters ($Cs^+(CH_3OH)_m$ or $Li^+(CH_3OH)_m$) and the solvated anion clusters ($Cl^-(CH_3OH)_m$) were efficiently decreased and increased, respectively. By the complexation of the cation with the crown ether, the cation−methanol interaction was controlled, whereas the anion−methanol interaction was promoted through the indirect effect, that is, the decrease of the electrostatic influence of the cation on the anion. Accordingly, the solvated anion clusters formed in the presence of crown ether reflect the intrinsic anion−methanol interaction. The intrinsic solvation for Cl^-, I^-, and ClO_4^- were compared by the measurements of their lithium salts in methanol including 18-crown-6. The observed solvated anion clusters had good relation with the free-energy change for solvation of anions by methanol.

Introduction

Ions in solution are vital to various physicochemical and biological processes; therefore, the salt effect on these processes has been extensively studied.[1−4] In relation with the study on microscopic origin of the salt effect, structures of solvated ions[5−7] have been investigated through experimental (X-ray diffraction,[8−12] NMR,[13−15] ion cyclotron resonance spectrometry,[16,17] etc.) and theoretical (molecular dynamics simulations[18−20] etc.) methods; however, the relation between the ion−solvent interaction and the ion−counterion interaction has not been studied experimentally. Ions in solution should have interactions with both solvent molecules and counterions; therefore, the change of the microscopic environment around an ion, caused by a kind of chemical reaction, will induce the change of the microscopic environment (solvation) around the counterion. Conversely, the solvation and the reactivity of an ion will be also dependent on the counterion.

Here we focus on the solvation structures of alkali metal salts (CsCl, LiCl, LiI, and $LiClO_4$) in methanol observed through mass spectrometric analyses of positive and negative ion clusters. Especially, we report the dynamic change of the solvations for ions and their counterions induced by the interaction of the cation with a crown ether (18-crown-6 (18C6)). The complementary relation between the ion−counterion interaction and the ion−solvent interaction is clearly demonstrated.

Experimental Section

The mass spectra of clusters isolated from electrolyte solutions were measured by the specially designed mass spectrometer using electrospray interface.[21] The sample solution was injected into five-stage differentially pumped vacuum system by an HPLC pump with a flow rate of 0.01 mL min^{-1} through a fused silica capillary tube (i.d. 0.1 mm). The high electric voltages were supplied to nozzle (±2.6∼2.9 kV) and skimmers (±230∼290 V) for the electrospray.[22,23] The positive and negative voltages were selected for measurement of positive and negative ion clusters, respectively. The multicharged liquid droplets including excess cations or anions were generated through this homemade electrospray interface, heated at 40 °C for assistance of the formation of spray against the decrease of the nozzle temperature. The resulting multicharged liquid droplets are led from the first chamber (760 Torr) to the second (10 Torr), third (0.01 Torr), fourth (10^{-5} Torr), and fifth chamber (10^{-6} Torr) through the pressure difference and a gradient of the electric field. During the flight of the liquid droplets, they are fragmented into clusters, molecules, or ions via adiabatic expansion and electrostatic repulsion. The formed clusters charged by included ions were analyzed in the fifth chamber (10^{-7} Torr) by a quadrupole mass spectrometer (Extrel C50) without any external ionization. The correlation between the observed cluster structures and intermolecular interactions in solution has been confirmed for the various solutions.[24−27] All chemicals were purchased from WAKO (Osaka, Japan) and were used as received.

Results and Discussion

Correlation of the Microscopic Environment of a Cation with That of Its Counteranion.

Figure 1 shows the mass spectra of positive ion clusters generated from methanol solutions including CsCl (1.0×10^{-3} mol dm^{-3}) and various amounts of 18-crown-6 (0∼1. 0×10^{-2} mol dm^{-3}). As for the CsCl solution without 18-crown-6 (Figure 1a), naked and solvated Cs^+ clusters ($Cs^+(CH_3OH)_m$; $m = 0∼5$) are observed dominantly, and CsCl salt clusters ($Cs^+(CsCl)_n$; $n = 1∼5$) also form considerably with including solvent methanol.

---

* To whom correspondence should be addressed. E-mail: akihiro-wakisaka@aist.go.jp.

[†] Research fellow of New Energy and Industrial Technology Development Organization, Japan.

10.1021/jp014583q CCC: $22.00

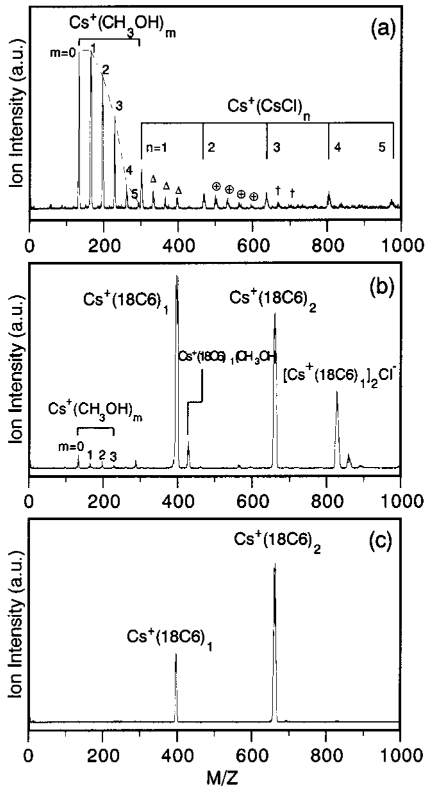

Figure 1. Positive-ion mass spectra of clusters generated from methanol solutions including CsCl (fixed concentration: 1.0×10^{-3} mol dm^{-3}) and 18C6 (variable concentration: (a) 0, (b) 1.0×10^{-3} mol dm^{-3}, (c) 1.0×10^{-2} mol dm^{-3}). Δ, ⊕, and † correspond to the solvated salt clusters, $Cs^+(CsCl)_n(CH_3OH)_m$ of $n = 1$, 2, and 3, respectively.

The naked Cs^+ ion was thought to be formed by evaporation of the methanol in the solvated Cs^+ clusters, $Cs^+(CH_3OH)_m$, during fragmentation of the liquid droplets. The salt clusters $Cs^+(CsCl)_n$ with $n = 1$, 2, and 3 have interaction with solvent methanol molecules, owing to higher charge density of smaller salt clusters, to form solvated salt clusters $Cs^+(CsCl)_n(CH_3OH)_m$. The solvated ions and the salt clusters are strongly influenced by the presence of an 18-crown-6. At the concentration of [18-crown-6] = [CsCl] = 1.0×10^{-3} mol dm^{-3} (Figure 1b), a 1:1 complex, $Cs^+(18C6)_1$, is observed as the most prominent species, and $Cs^+(18C6)_2$ and $[Cs^+(18C6)_1]_2Cl^-$ are also observed dominantly, with decrease of the naked Cs^+, solvated Cs^+, and salt clusters observed in Figure 1a. The formation of a 1:2 complex, $Cs^+(18C6)_2$, is due to (Cs^+ diameter (3.6 Å)) > (cavity diameter of 18-crown-6 (2.6∼3.2 Å)), which is in good contrast with the case that LiCl is used instead of CsCl as described later. The $[Cs^+(18C6)_1]_2Cl^-$ is formed through the interaction of two $Cs^+(18C6)_1$ with Cl^-, that is, the Cl^- will be sandwiched by two $Cs^+(18C6)_1$. With increase of the 18-crown-6 concentration, at the concentration of 18-crown-6 10 times higher than that of CsCl (Figure 1c), the formation of $Cs^+(18C6)_2$ overwhelms that of $Cs^+(18C6)_1$. This indicates that the consecutive equilibrium for complex formation shifts to the right-hand as follows:

$$Cs^+ + 18C6 \rightarrow Cs^+(18C6)_1$$

$$Cs^+(18C6)_1 + 18C6 \rightarrow Cs^+(18C6)_2$$

which leads to the decrease of $Cs^+(18C6)_1$.

Figure 1 clearly shows that the microscopic environment around Cs^+ in methanol changes drastically with varying the concentration of 18-crown-6. Without 18-crown-6, Cs^+ have interaction with not only the solvent methanol but also the counterion Cl^-, as given by the formation of $Cs^+(CH_3OH)_m$ and $Cs^+(CsCl)_n$ in Figure 1a. This indicates that the microscopic environments of Cs^+ are determined by the balance between the solvation by the methanol and the Coulombic force with Cl^-. With increasing the concentration of 18-crown-6, the complexation of Cs^+ with two molecules of 18-crown-6 becomes free from the interactions of Cs^+ with methanol and Cl^-, which corresponds to the drastic change of microscopic environment around Cs^+.

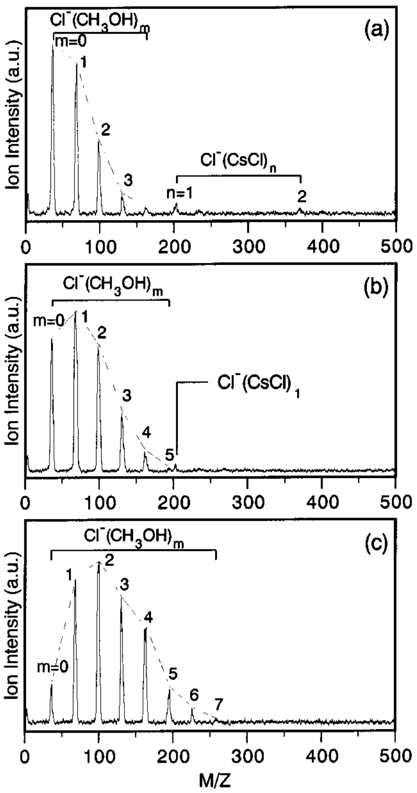

Figure 2. Negative-ion mass spectra of clusters generated from methanol solutions including CsCl (fixed concentration: 1.0×10^{-3} mol dm^{-3}) and 18C6 (variable concentration: (a) 0, (b) 1.0×10^{-3} mol dm^{-3}, (c) 1.0×10^{-2} mol dm^{-3}).

Here, it was first observed that the change of the microscopic environment around the positive ion affected the microscopic environment of the negative ion consequently. The measurement of the negative ion clusters demonstrated how the solvation for Cl^- was influenced by the change of the microscopic environment around Cs^+.

Figure 2 shows the mass spectra of negative ion clusters generated from the same solution as used in the measurement of the positive ion clusters (Figure 1). Figure 1a, 1b, and 1c corresponds to Figure 2a, 2b, and 2c, respectively; one is positive side and the other is negative side. As for pure CsCl solution without 18-crown-6 (Figure 2a), naked and solvated Cl^- ($Cl^-(CH_3OH)_m$; $m = 0$∼4) are observed as a series of clusters. The naked Cl^-, $m = 0$, will be formed from solvated Cl^- through vaporization, and this intensity is related to the solvation energy, as described later. The salt clusters ($Cl^-(CsCl)_n$; $n = 1$, 2) are also observed similar to ones in the positive ion cluster measurement (Figure 1a). In the presence of 18-crown-6, the solvation of Cl^- by the methanol is enhanced remarkably (Figure 2b). With increasing the 18-crown-6 concentration, the solvated Cl^-, $Cl^-(CH_3OH)_m$ with $m = 1$∼7, becomes more favorable as shown in Figure 2c.

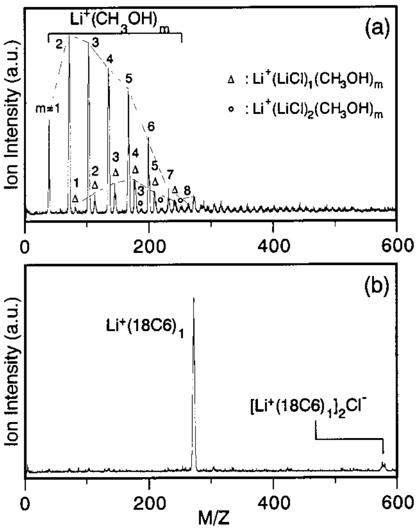

Figure 3. Positive-ion mass spectra of clusters generated from methanol solutions including LiCl (fixed concentration: 1.0×10^{-3} mol dm^{-3}) and 18C6 ((a) 0, (b) 1.0×10^{-2} mol dm^{-3}). The numbers shown above the peaks represent the number of methanol (m) of $Li^+(CH_3OH)_m$ and $Li^+(LiCl)_n(CH_3OH)_m$.

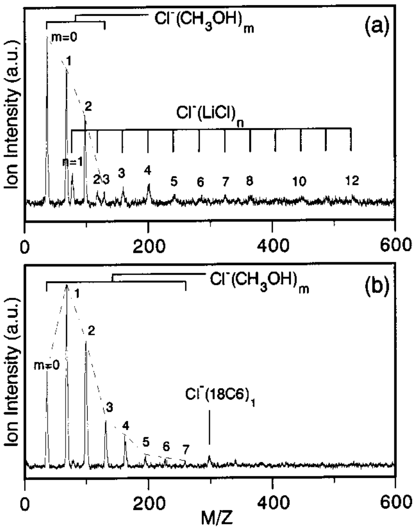

Figure 4. Negative-ion mass spectra of clusters generated from methanol solutions including LiCl (fixed concentration: 1.0×10^{-3} mol dm^{-3}) and 18C6 ((a) 0, (b) 1.0×10^{-2} mol dm^{-3}).

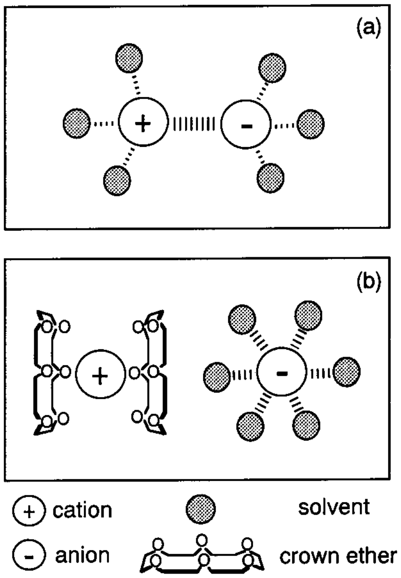

Figure 5. Schematic picture for microscopic environment of an ion and its counterion. (a) In solution including cation and counteranion, solvation and Coulombic force are balanced. (b) In the presence of a crown ether, the balance shown in (a) is broken to reorganize the microscopic environment.

With increasing the concentration of 18-crown-6, Cs^+ interacts with 18-crown-6 preferentially, as shown in Figure 1. This prevents the Cs^+ from interacting with the Cl^-. In other words, the Cl^- becomes free from the Coulombic force with Cs^+ in the presence of enough 18-crown-6, and its negative charge should be stabilized mainly through the solvation. This causes the enhancement of solvation for Cl^-. This indicates that there is complementary relation between the ion−counterion interaction and the ion (or counterion)−solvent interaction.

The same complementary relation was confirmed for the case that LiCl was used instead of CsCl. Figure 3 shows the mass spectra of positive ion clusters generated from methanol solutions including LiCl (1.0×10^{-3} mol dm^{-3}) in the presence and absence of 18-crown-6. As for LiCl solution without 18-crown-6 (Figure 3a), solvated Li^+ clusters ($Li^+(CH_3OH)_m$; $m = 1{\sim}8$) are observed dominantly, and LiCl salt clusters exist with including solvent methanol, $Li^+(LiCl)_n(CH_3OH)_m$, as shown in the CsCl system similarly. In comparison with Cs^+, the solvations for Li^+ and the salt clusters are more preferable because of higher charge density of Li^+ than that of Cs^+. In the presence of excess amount of 18-crown-6 over Li^+ (Figure 3b), $Li^+(18C6)_1$ is observed predominantly with disappearing the solvated Li^+ and salt clusters. The complexation of Li^+ with 18-crown-6 is quite different from that of Cs^+, that is, the size of Li^+ smaller than the cavity size of 18-crown-6 allows to form only a 1:1 complex even at a higher concentration of 18-crown-6.

Such a change of microscopic environment of Li^+ led to the change of the microscopic environment of the Cl^-, as demonstrated for the CsCl system. As for LiCl solution without 18-crown-6 (Figure 4a), naked and solvated Cl^- and LiCl salt clusters are observed similar to the CsCl system (Figure 2a).[28] In the presence of the excess amount of 18-crown-6, the solvation for Cl^- is obviously promoted with disappearing the salt clusters (Figure 4b).

Figure 5 shows schematic illustration on the solvation for the ion and the counterion controlled by the external influence (the addition of crown ether in this case). The original solvation structures of cation and anion are determined by the balance between Coulombic force with the counterion and the affinity to the solvent (Figure 5a). In the presence of a crown ether as an external influence, the complexation of the cation with the crown ether shields the Coulombic force with the counterion. This increases the solvation for anion to complement the decrease of the Coulombic interaction with the countercation (Figure 5b).

Although the crown ether does not interact with Cl^- directly, the solvation for Cl^- is enhanced considerably with increase of the crown ether concentration. Such an indirect effect on the solvation should be recognized as one of the inherent properties of solution. In this sense, the clusters observed here reflect the microscopic interactions in the solution.

To see how the observed clusters reflect the microscopic environment in a solution, here we would like to compare cluster structures observed through the mass spectrometry with the molar conductivity. As shown in Figures 1a, 2a, 3a, and 4a, the salt clusters such as $Cs^+(CsCl)_n$ and $Li^+(LiCl)_n$ are formed from methanol solutions without 18-crown-6, which suggests that the interaction of Cs^+ and Li^+ with Cl^- is considerable to

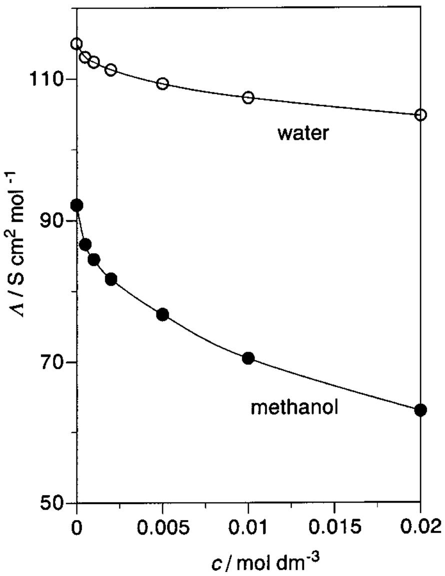

Figure 6. Molar conductivities of LiCl in water and methanol at 298 K as a function of LiCl concentration. Λ: molar conductivity, *c*: concentration of LiCl.

form ion pairs in methanol. This ion-pair formation in methanol should have strong relation with the molar conductivity.[29] Figure 6 shows the molar conductivities of LiCl in water and methanol as a function of the LiCl concentration.[30] The molar conductivity for the aqueous solution is nearly constant with increasing the concentration, which means that LiCl in water behaves like a typical strong electrolyte that almost dissociates to Li^+ and Cl^- even at higher concentrations. On the other hand, one for the methanol solution decreases more rapidly with increasing the concentration, which means that the electrolytic dissociation efficiency for LiCl in methanol decreases markedly with increasing the concentration, because of Li^+Cl^- ion-pair or salt-cluster $Li^+(LiCl)_n$ formation. Assuming that the ratio of molar conductivity at a concentration of one at infinite dilution reflects the ratio of electrolytic dissociation in solution, the electrolytic dissociation efficiency in methanol at [LiCl] = 1.0×10^{-3} mol dm^{-3}, where the mass spectra were measured, will be calculated to be 90.7% by using the values plotted in Figure 6. The remaining 9.3% of LiCl will exist as ion pairs or salt clusters corresponding to nonionized LiCl, which do not contribute to the conductivity.

The ratio of nonionized LiCl in methanol can be also estimated through the peak intensities of cluster observed in the mass spectrum (Figure 3a), as represented by R_{SALT} in eq 1.

$$R_{\mathrm{SALT}} = \frac{\Sigma \mathrm{Li}_{\mathrm{bound}}}{\Sigma \mathrm{Li}_{\mathrm{bound}} + \Sigma \mathrm{Li}_{\mathrm{free}}} \qquad (1)$$

where $\Sigma\mathrm{Li}_{\mathrm{bound}}$ and $\Sigma\mathrm{Li}_{\mathrm{free}}$ represent the number of Li^+ bound to Cl^- and the number of free Li^+ released from LiCl, respectively. In the clusters observed in Figure 3a, the solvated salt clusters, $Li^+(LiCl)_n(CH_3OH)_m$, include nLi^+ bound to nCl^-; therefore, $\Sigma\mathrm{Li}_{\mathrm{bound}}$ is expressed by eq 2. Since each peak observed as $Li^+(CH_3OH)_m$ and $Li^+(LiCl)_n(CH_3OH)_m$ in Figure 3a includes a free Li^+ released from LiCl, $\Sigma\mathrm{Li}_{\mathrm{free}}$ is expressed by eq 3.

$$\Sigma\mathrm{Li}_{\mathrm{bound}} = n\sum_{n}\sum_{m} I\mathrm{Li}^+(\mathrm{LiCl})_n(\mathrm{CH_3OH})_m \qquad (2)$$

$$\Sigma\mathrm{Li}_{\mathrm{free}} = \sum_{m} I\mathrm{Li}^+(\mathrm{CH_3OH})_m + \sum_{m}\sum_{n} I\mathrm{Li}^+(\mathrm{LiCl})_n(\mathrm{CH_3OH})_m \qquad (3)$$

where $\sum_m\sum_n I\mathrm{Li}^+(\mathrm{LiCl})_n(\mathrm{CH_3OH})_m$ and $\sum_m I\mathrm{Li}^+(\mathrm{CH_3OH})_m$ represent the sum of the peak intensities of $Li^+(LiCl)_n(CH_3OH)_m$

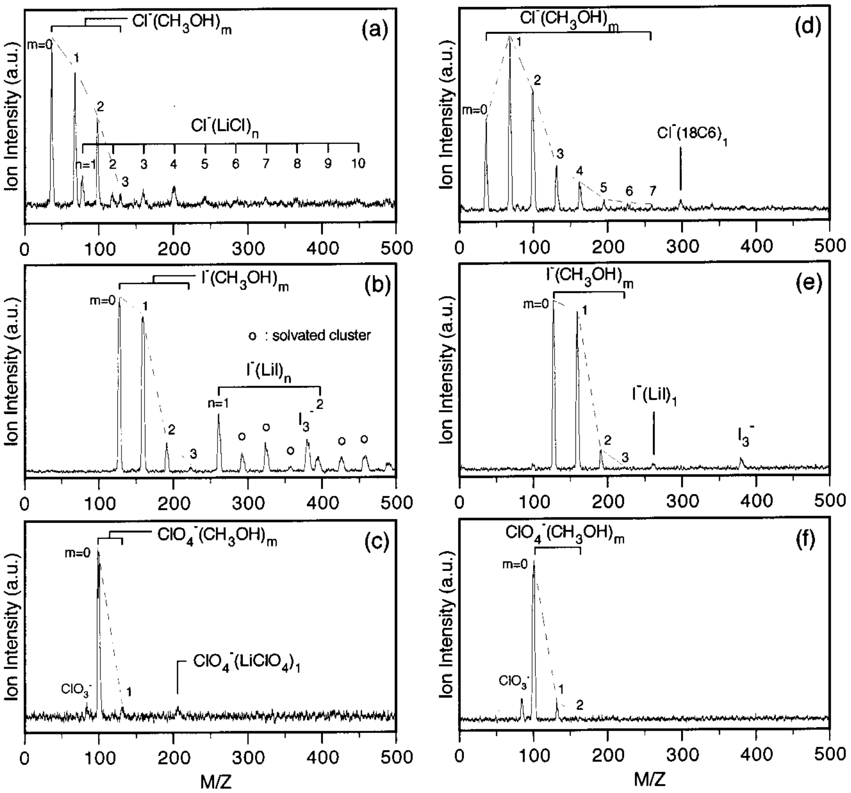

Figure 7. Negative-ion mass spectra of clusters generated from methanol solutions including lithium salt (1.0×10^{-3} mol dm^{-3}) without 18C6 (1.0×10^{-2} mol dm^{-3}) ((a) LiCl, (b) LiI, and (c) $LiClO_4$) and with 18C6 ((d) LiCl, (e) LiI, and (f) $LiClO_4$). (a) and (d) are the same data as Figure 4. In the absence of 18C6 ((a), (b), and (c)), the observations of the salt clusters such as $Cl^-(LiCl)_n$, $I^-(LiI)_n$, and $ClO_4^-(LiClO_4)_1$ indicate a existence of the interaction between cation and anion in solution.[32]

TABLE 1: Free Energies of Solvation of Ions by Methanol (1 atm Gas → Unit Mol Fraction Solution): ΔG_{Sol} in kJ mol^{-1} at 298K[a]

anion	ΔG_{sol}
Cl^-	−270.7
Br^-	−244.3
I^-	−211.3
ClO_4^-	−188.3

[a] Reference 31.

and $Li^+(CH_3OH)_m$ observed in Figure 3a, respectively. Thus, the R_{SALT} value was calculated through eqs 1, 2, and 3. The resulting R_{SALT} at [LiCl] = 1.0×10^{-3} mol dm^{-3} in methanol was 0.158 (15.8%), which indicates that 15.8% of 1.0×10^{-3} mol dm^{-3} LiCl exist as ion pairs or salt clusters.

The resulting value (15.8%) is larger than the value calculated from the molar conductivity (9.3%); however, there is a good correlation between these values, in consideration of the vaporization of solvent methanol to increase the concentration, during the fragmentation of liquid droplets into clusters. This correlation indicates that ion pairs or salt clusters are formed besides solvated ions in the methanol solutions. Moreover, the ion−counterion interaction in methanol observed through the mass spectrometry will be reasonable.

Solvated Anions without Influence of the Countercations. It is thought that the observed solvated Cl^- clusters ($Cl^-(CH_3OH)_m$) in the presence of the excess amount of the 18-crown-6 over the existing cation (Cs^+ or Li^+) reflect a kind of intrinsic anion−solvent interaction because the complexation of the cation with the crown ether efficiently shields the electrostatic influence on the counteranion. This suggests that the anion−solvent interaction without electrostatic influence of the cation can be measured in the presence of crown ether.

To compare the intrinsic anion−solvent interactions for Cl^-, I^-, and ClO_4^-, the mass spectra of negative ion clusters generated from methanol solutions of LiCl, LiI, and $LiClO_4$ were compared with those in the presence of 18-crown-6. Figure 7a, 7b, and 7c shows negative ion mass spectra of LiCl, LiI, and $LiClO_4$ in methanol without including 18-crown-6, respectively. Figure 7a is the same as Figure 4a. Solvated Cl^-, $Cl^-(CH_3OH)_m$: $m = 1$, 2, and 3, is observed as a series of clusters, but solvated I^- and ClO_4^- become less favorable with increase of the ion radius.

The mass spectra of solvated Cl^-, I^-, and ClO_4^- in the presence of 18-crown-6 are shown in Figure 7d, 7e, and 7f, respectively. The solvation for Cl^- is obviously enhanced by the addition of 18-crown-6, as compared between Figure 7a and 7d. On the other hand, the solvations for I^- and ClO_4^- are not enhanced by the addition of 18-crown-6, as shown by comparison between Figure 7b and 7e and between Figure 7c and 7f. Such difference can be explained by solvation energy and Coulombic force depending on the ion radius. The reported free energies of solvation of Cl^-, Br^-, I^-, and ClO_4^- by methanol are listed in Table 1.[31] The stabilization of ions by the solvation is remarkably decreased with increasing size of ion. In comparing the intrinsic solvation of anions, Cl^-, I^-, and ClO_4^-, observed in Figure 7d, 7e, and 7f, the solvated I^- can be recognized but the solvated ClO_4^- are hardly observed. This indicates that the solvated ion having the change of free energies of solvation larger than around 200 kJ mol^{-1} ($|\Delta G_{\mathrm{sol}}| \geq 200$ kJ mol^{-1}) can remain as solvated ion and that less stable ones are fragmented into naked ions and solvent molecules. In Figure 7, the ion with smaller stabilization energy of solvation ($|\Delta G_{\mathrm{sol}}|$) forms its naked ion more abundantly. Furthermore, the solvation for the anions with smaller $|\Delta G_{\mathrm{sol}}|$, such as I^- and ClO_4^-, is not enhanced by the addition of 18-crown-6 because Coulombic interaction of these relatively large anions is too small to influence their solvation structure, which affords solvated ions close to the intrinsic structure even in the absence of 18-crown-6.

The correlations of our mass spectrometric analyses with the solvation energy and the aforementioned molar conductivity suggest that the cluster structures observed here are related to ion−solvent and ion−counterion interactions in solutions.

Conclusion

Solvation structures of positive and negative ions were determined by mass spectrometric analyses for alkali metal salts in methanol, which confirmed mutual influence between a microscopic environment of an ion and that of its counterion. In methanol solutions including alkali metal salts, solvation for the anion was promoted by the complexation of the cation with a crown ether. The increase of solvation for the anion compensates for the decrease of the electrostatic interaction to the anion caused by the cation-18-crown-6 complexation. The complementary relation between the ion−counterion and the ion−solvent interaction observed here is an intrinsic property of solution.

References and Notes

(1) Brendel, M. L.; Sandler, S. I. *Fluid Phase Equilib.* **1999**, *165*, 87.

(2) Jain, N. J.; George, A.; Bahadur, P. *Colloids Surf., A* **1999**, *157*, 275.

(3) Gundersen, S. A.; Sæther, Ø.; Sjöblom, J. *Colloids Surf., A* **2001**, *186*, 141.

(4) Desai, P. R.; Jain, N. J.; Sharma, R. K.; Bahadur, P. *Colloids Surf., A* **2001**, *178*, 57.

(5) Ohtaki, H.; Radnai, T. *Chem. Rev.* **1993**, *93*, 1157.

(6) Varadarajan, T. K.; Ramakrishna, T. V.; Kalidas, C. *J. Chem. Eng. Data* **1998**, *43*, 527.

(7) Lanza, G.; Fragalà, I. L.; Marks, T. J. *J. Am. Chem. Soc.* **2000**, *122*, 12764.

(8) Näslund, J.; Persson, I.; Sandström, M. *Inorg. Chem.* **2000**, *39*, 4012.

(9) Inada, Y.; Hayashi, H.; Sugimoto, K.; Funahashi, S. *J. Phys. Chem. A* **1999**, *103*, 1401.

(10) Díaz-Moreno, S.; Munoz-Páez, A.; Marcos, E. S. *J. Phys. Chem. B* **2000**, *104*, 11794.

(11) Tsutsui, Y.; Sugimoto, K.; Wasada, H.; Inada, Y.; Funahashi, S. *J. Phys. Chem. A* **1997**, *101*, 2900.

(12) Stålhandske, C. M. V.; Persson, I.; Sandström, M.; Kamienska-Piotrowicz, E. *Inorg. Chem.* **1997**, *36*, 3174.

(13) Kanakubo, M.; Ikeuchi, H.; Sata, G. P.; Yokoyama, H. *J. Phys. Chem. B* **1997**, *101*, 3827.

(14) Lucht, B. L.; Bernstein, M. P.; Remenar, J. F.; Collum, D. B. *J. Am. Chem. Soc.* **1996**, *118*, 10707.

(15) Fraenkel, G.; Duncan, J. H.; Wang, J. *J. Am. Chem. Soc.* **1999**, *121*, 432.

(16) Jarek, R. L.; Miles, T. D.; Trester, M. L.; Denson, S. C.; Shin, S. K. *J. Phys. Chem. A* **2000**, *104*, 2230.

(17) Jarek, R. L.; Shin, S. K. *J. Am. Chem. Soc.* **1997**, *119*, 10501.

(18) Balbuena, P. B.; Johnston, K. P.; Rossky, P. J. *J. Phys. Chem.* **1996**, *100*, 2706.

(19) Chang, T.-M.; Dang, L. X. *J. Phys. Chem. B* **1997**, *101*, 10518.

(20) Torii, H. *J. Phys. Chem. A* **1999**, *103*, 2843.

(21) Wakisaka, A.; Watanabe, Y. *J. Phys. Chem. B* **2002**, *106*, 899.

(22) Fenn, J. B.; Rosell J.; Meng, C. K. *J. Am. Soc. Mass Spectrom.* **1997**, *8*, 1147.

(23) Kebarle, P.; Peschke, M. *Anal. Chim. Acta* **2000**, *406*, 11.

(24) Wakisaka, A.; Yamamoto, Y. *J. Chem. Soc., Chem. Commun.* **1994**, 2105.

(25) Wakisaka, A.; Yamamoto, Y.; Akiyama, Y.; Takeo, H.; Mizukami, F.; Sakaguchi, K. *J. Chem. Soc., Faraday Trans.* **1996**, *92*, 3339.

(26) Wakisaka, A.; Akiyama, Y.; Yamamoto, Y.; Engst, T.; Takeo, H.; Mizukami, F.; Sakaguchi, K.; Jones, H. *J. Chem. Soc., Faraday Trans.* **1996**, *92*, 3539.

(27) Mochizuki, S.; Usui, Y.; Wakisaka, A. *J. Chem. Soc., Faraday Trans.* **1998**, *94*, 547.

(28) The formation of $Cl^-(LiCl)_n$ is more efficient than that of $Cl^-(CsCl)_n$, which is attributed to the strong interaction between Li^+ and Cl^-, on the basis of the higher charge density of Li^+. The salt clusters with negative charge are hardly solvated, but ones with positive charged are markedly solvated. This can be related with the charge density of ions in

$Li^+(LiCl)_n$ and $Cl^-(LiCl)_n$: the former is the higher. Additionally, the affinity of Cl^- to methanol is not as high as that of Li^+, then the addition of solvent methanol to $Cl^-(LiCl)_n$ is not effective.

(29) Kobara, H.; Wakisaka, A.; Takeuchi, K.; Ibusuki, T. *J. Phys. Chem. A* **2002**, *106*, 4779.

(30) (a) *Landolt-Börnstein Tabelen*, II Band, 7 Teil, Elektrische Eigenschaften II; Springer-Verlag: Berlin, 1960; p 34∼82, 353. (b) Washburn, E. W. *International Critical Tables*; McGraw-Hill: New York, 1949; Vol. VI, p 231∼255. (c) Robinson, R. A.; Stokes, R. H. *Electrolyte Solutions*; Butterworths: London, 1959; p 162.

(31) Abraham, M. H.; Liszi, J. *J. Chem. Soc., Faraday Trans. 1* **1978**, *74*, 1604.

(32) Formations of ClO_3^- and I_3^- as an electrochemical side reaction of the electrospray cannot be eliminated.